Available online at www.sciencedirect.com

ScienceDirect

Procedia Structural Integrity 7 (2017) 368–375

Structural Integrity Procedia

www.elsevier.com/locate/procedia

3rd International Symposium on Fatigue Design and Material Defects, FDMD 2017, 19-22 September 2017, Lecco, Italy

Evaluation of Size Effect in Low Cycle Fatigue for Q&T rotor steel

S.P. Zhu[a, b, *], S. Foletti[b], S. Beretta[b]

[a]School of Mechatronics Engineering, University of Electronic Science and Technology of China, Chengdu 611731, China
[b]Department of Mechanical Engineering, Politecnico di Milano, Via La Masa 1, 20156 Milan, Italy

Abstract

This study presents a probabilistic modeling of size effect of 30NiCrMoV12 steel in a low cycle fatigue (LCF) regime. Three types of fatigue tests have been conducted on three geometrical specimens. Results indicate that nearly all of the LCF lifetime of 30NiCrMoV12 consists of the development of multiple surface short cracks, which has shown statistical aspects of their mutual interactions and coalescence. This gives rise to an approach of LCF damage based on statistical physics. A statistical Weibull's weakest link model has been verified and a procedure for surface multiple fracture simulation is then established by including the random processes of initiation, propagation and coalescence of dispersed surface cracks. Using this procedure, the life of a component can be predicted from the criterion of critical cracks formation by coalescence of dispersed defects.

Peer-review under responsibility of the Scientific Committee of the 3rd International Symposium on Fatigue Design and Material Defects.

Keywords: size effect; low cycle fatigue; crack growth; statistics of extremes; crack coalescence

1. Introduction

Fatigue and fracture tests are normally conducted on small test specimens of structural materials used for aircrafts and high-speed trains. In predicting the fatigue life of full scale components or structures, such as high speed train railway axles, the specimen size effect is critical when utilizing the laboratory testing of small standard specimens as the reference basis. In other words, fatigue testing on large specimens for those structures is not always possible due to financial considerations. Therefore, characterizing the effect of specimen size on fatigue life is needed and corresponding methods are lacking, especially a robust probabilistic method for quantifying the effect of specimen size on fatigue life.

According to the German FKM guideline launched for the strength assessment of structures under different loading conditions, the treatment of size effect is purely empirical, which is determined from empirical design curves or formulae [1-3]. The application of this size effect to other cross-sectional shapes and stress distributions is often not explained as well as the robustness of the low cycle fatigue (LCF) resistance against specimen size [4]. One of the commonly-used way to characterize the size effect by means of the weakest-link theory and the statistics of extremes. Therefore, to explain the specimen size effect toward increasing reliability of fatigue critical components, metallurgical and mechanical details must be considered in fatigue modelling and lifing procedure. Note from [5, 6] that LCF life of ductile steels is generally dominated by crack propagation life rather than crack initiation life. Namely, the effect of specimen size on the fatigue propagation rate, particularly on the scatter in small fatigue crack growth, has been viewed as the main factor influencing the fatigue life. The challenge will be to use not only the governing factors, such as

* Corresponding author. *E-mail address:* zspeng2007@uestc.edu.cn

Peer-review under responsibility of the Scientific Committee of the 3rd International Symposium on Fatigue Design and Material Defects.
10.1016/j.prostr.2017.11.101

local microstructure, local stress/strain, and damage physics, but also statistical approaches to understand the size effect in a LCF regime. According to this, this paper attempts to quantify the specimen size effect on fatigue lives of 30NiCrMoV12 steel from the viewpoint of mechanical-probabilistic modelling and numerical simulation of fatigue crack growth. In this paper, an alternative procedure for practical fatigue design by considering size effect will be critically investigated.

2. Experimental

2.1. Material

Low cycle fatigue tests have been conducted on specimens with three different geometries of similar shape, which are designed according to ASTM standard E606 [7] and prepared by electro-chemical polishing [8]. Figure 1 shows one of the specimen geometries used for the LCF tests. Three different specimen geometries have been manufactured to study statistical size effects. The diameter (D_0) and the gauge length (L_0) of the specimen are listed in Table 1. The specimens were made of 30NiCrMoV12 steel, which is commonly used for railway axles due to high mechanical properties and high performance. Its heat treatment includes normalization at 900℃ for uniforming and grain size refinement, then a quench treatment at 850℃ and cooling in oil bath, finally a tempering process taking at 625℃ for 12 hours in order to increase toughness. Monotonic mechanical properties of 30NiCrMoV12 are reported in Table 2.

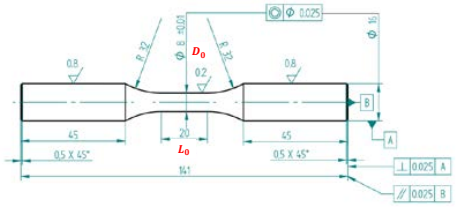

Figure 1. Standard specimen geometry for LCF tests

Table 1. Three specimen geometries

Geometry	D_0/mm	L_0/mm
G1: Standard	8	20
G2: Small	3	8
G3: Large	14	36

Table 2. Mechanical properties of 30NiCrMoV12

Elastic modulus E	$197GPa$
Yield stress σ_y	$878MPa$
Ultimate tensile strength σ_{UTS}	$1045MPa$
Elongation at fracture	21.6%

2.2. Testing

For the investigation of LCF lifetime behaviour, MTS fatigue testing machines with maximum loads of 100 kN and 250 kN have been used for tension-compression testing. The strain range was controlled by three extensometers. All LCF tests were carried out at strain amplitude levels between 0.35% and 0.8% at load ratio $R = -1$. Fatigue lifetime of the specimen is defined according to the load drop criterion. In this analysis, three types of LCF tests were performed, including typical LCF tests and replica tests on smooth/notched specimens. The latter were conducted to observe the crack length for crack growth/evolution modelling on the specimen surface, particularly, some tension-compression tests were interrupted at fixed cycles and plastic replicas of the specimen surfaces were made. The quantitative crack length and numbers were determined by optical microscopy. All replica tests were performed on smooth and notched standard specimens at strain amplitude $\varepsilon_a = 0.5\%$. For the notched standard specimen, two micro holes of $100\mu m$ diameter were drilled with an angular distance of $120°$ and 1.5 millimeter far from the centre line of the specimen. Replicas were taken during three tests on the standard specimens, three tests on the big specimen and six interrupted tests for the small specimens. In this study, the surface cracks with length longer than $20\mu m$ were measured for statistical analysis.

2.3. Results

In LCF analysis, a so-called strain-life approach, like the Coffin-Manson (CM) equation, is often used to describe the relationship between strain and the number of cycles to failure under uniaxial loadings, which relates the local elastic-plastic behaviour by

$$\frac{\Delta\varepsilon_t}{2} = \frac{\Delta\varepsilon_e}{2} + \frac{\Delta\varepsilon_p}{2} = \frac{\sigma_f'}{E}\left(2N_f\right)^b + \varepsilon_f'\left(2N_f\right)^c \tag{1}$$

where $\Delta\varepsilon_t, \Delta\varepsilon_e$ and $\Delta\varepsilon_p$ are the total strain range, elastic strain range and plastic strain range, respectively; σ_f' is the fatigue strength coefficient; E is the Young's modulus; N_f is the number of cycles to failure; b is the fatigue strength exponent; ε_f' is the fatigue ductility coefficient; c is the fatigue ductility exponent.

When using Eq. (1) for LCF analysis, the Ramberg-Osgood (RO) equation described the stress-strain behaviour of the material

$$\frac{\Delta\varepsilon_t}{2} = \frac{\Delta\varepsilon_e}{2} + \frac{\Delta\varepsilon_p}{2} = \frac{\Delta\sigma}{2E} + \left(\frac{\Delta\sigma}{2K'}\right)^{\frac{1}{n'}} \tag{2}$$

where $\Delta\sigma$ is the tress range; K' and n' are the cyclic strength coefficient and cyclic strain hardening exponent, respectively.

Using Eq. (1) and Eq. (2), cyclic response and fatigue behaviour of three specimen sizes can be plotted as shown in Figure 2.

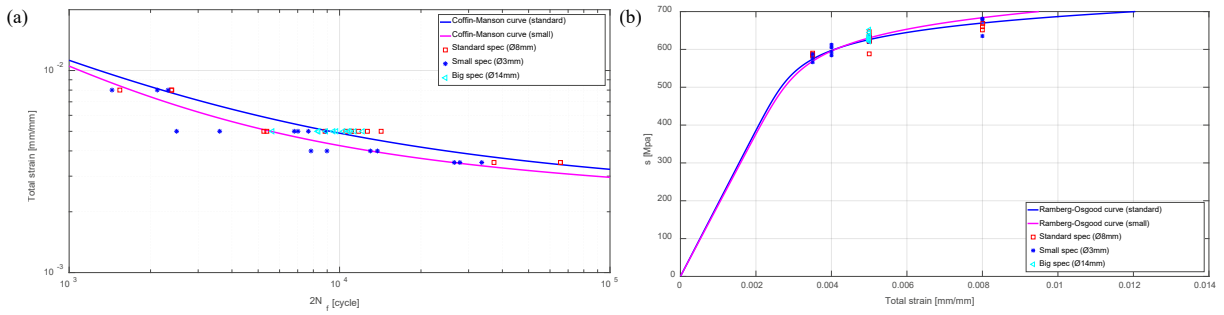

Figure 2. LCF tests of three different specimens of 30NiCrMoV12

3. Size effect in LCF based on weakest-link modeling

3.1. Weakest-link theory

The weakest link theory was originally developed by Weibull to describe the tensile fracture of brittle materials, which is based on the Weibull probability distribution of failure. Specifically, due to the randomly distributed material defects (non-homogeneities, inclusions, precipitates) in a material per volume unit, the theory states that fatigue crack initiates where the most dangerous defect or the weakest link exists [4, 9, 10]. Thus, a stochastic distribution of defects within specimens/components leads to scatter in the fatigue behaviour of the material. Through relating the effect of load and cross-sectional area with the fatigue life, a classic form of the Weibull distribution for the failure probability can be expressed as

$$P_f(\sigma,\Omega) = 1 - exp\left[-\frac{1}{\Omega_0}\int_\Omega f(\sigma)d\Omega\right] \tag{3}$$

where Ω_0 is the reference volume or surface; $f(\sigma)$ is a function of the risk of rupture with three parameters

$$f(\sigma) = \left(\frac{\sigma-\sigma_u}{\sigma_0}\right)^m \tag{4}$$

where m and σ_0 are the shape parameter and scale parameter of the Weibull distribution, respectively; σ_u is the threshold stress.

By using Eq. (3) for describing the life (as done by Wormsen et al. [10]), the distribution of experimental results can be derived for specimens with different geometries. By increasing the component volume or surface, the probability of failure increases due to the higher probability of finding a critical defect. Thus, a relation can be obtained for two different specimen sizes under a similar failure probability

$$\frac{N_2}{N_1} = \left(\frac{A_1}{A_2}\right)^{\frac{1}{m}} \tag{5}$$

where N_1 is the fatigue life for a specimen with the known surface or cross-sectional area A_1, N_2 is the estimated fatigue life for the specimen with determined surface or cross-sectional area A_2. In the current research, A_1 and A_2 can be calculated over the gage section of different specimens.

Adopting Eq. (5) and taking the distribution of fatigue life of small specimens as a reference, the distribution of the life for large and standard specimens can be expressed by a function of the probability of failure of small specimens $P_{f,small}$ as

$$P_{f,standard} = 1 - \left[1 - P_{f,small}\right]^{\eta_{standard}} \tag{6}$$

$$P_{f,large} = 1 - \left[1 - P_{f,small}\right]^{\eta_{large}} \tag{7}$$

where $\eta_{standard}$ and η_{large} are the ratio between gauge surfaces of the standard/large specimens and the small ones, respectively.

Under a log-normal life distribution of different sizes of specimens, Figure 3 plots life distributions of the standard and large specimens according to Eq. (6) and Eq. (7). Comparing with experimental mean and scatter of the life cycles at $\epsilon_a = 0.5\%$, a consequence of the defects distribution based on statistic of extremes cannot explain well the tested life distributions in Figure 3.

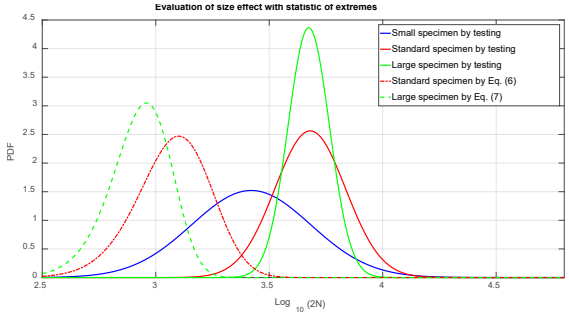

Figure 3. Expected life based only on size effect due to statistic of extremes

3.2. Fatigue crack growth life

Note from Figure 4 that the inspection of fracture surfaces with SEM show that most cracks initiated at the surface of the specimen. For 30NiCrMoV12 steel, its LCF life is obviously dominated by crack propagation life rather than crack initiation life. Thus, the effect of specimen geometrical size on the fatigue crack propagation rate is critical essential for a theoretical understanding of fatigue lives.

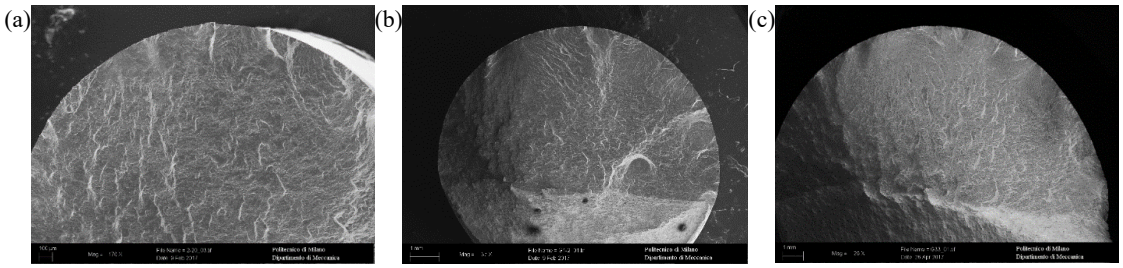

Figure 4. Multiple surface cracks of (a) small, (b) standard and (c) large specimen

Fatigue crack growth in the presence of a marked plastic strain range under LCF conditions can be well described by using Tomkins model [11]. Through assuming the amount of crack growth per cycle under tension-compression loadings to be the amount of irreversible shear decohesion which occurs at the crack tip, Tomkins [11] correlates crack growth to the plastic strain amplitude in an exponential law

$$\begin{cases} a = a_i e^{k_g N} \\ k_g = k_{g0} \varepsilon_{pa}^{d} \end{cases} \tag{8}$$

where a and a_i are the crack length and initial crack length, respectively; ε_{pa} is the plastic strain amplitude, k_{g0} and d are material parameters that establish the short cracks growth in a material.

Accordingly, a simplified form can be expressed as

$$\frac{da}{dN} = k_g a \tag{9}$$

The number of cycles is obtained by integrating Eq. (9) from an initial crack length a_i to a final one a_f. Parameter of Eq. (9) was calibrated from experiments, as shown in Figure 5. Two scale factors can be obtained to shift the distribution found with the statics of extremes for the standard/large specimen from the reference small one

$$\gamma_{standard} = \frac{\Delta N_{standard}}{\Delta N_{small}} = \frac{ln\left(\frac{log_{10}(a_f,standard)}{log_{10}(a_i)}\right)}{ln\left(\frac{log_{10}(a_f,small)}{log_{10}(a_i)}\right)} \tag{10}$$

$$\gamma_{large} = \frac{\Delta N_{large}}{\Delta N_{small}} = \frac{ln\left(\frac{log_{10}(a_f,large)}{log_{10}(a_i)}\right)}{ln\left(\frac{log_{10}(a_f,small)}{log_{10}(a_i)}\right)} \tag{11}$$

Combining Eq. (6) to Eq. (11), the life scale factors at $\epsilon_a = 0.5\%$ due to the propagation size effect can be calculated from an initial crack length $a_i = 100\mu m$ to a final crack length $a_f = \frac{\pi D_0}{2}$, namely, $\gamma_{standard} = 1.18048$ and $\gamma_{large} = 1.27523$.

As pointed out by Koyama et al. [5], the specimen size effect can be quantified by the sum of the effect of statistical distribution

of the defects and the effect of crack propagation. From a crack growth point of view, a larger specimen would lead to a longer life, which shift the dotted/dash lines in Figure 3 to the right-hand of the *x*-axis. According to this, a comparison between the curves of experimental distribution of the life and the ones due to the effects of statistical defects and crack propagation can be made by using Eq. (10) and Eq. (11), as shown in Figure 6 and results in Table 3.

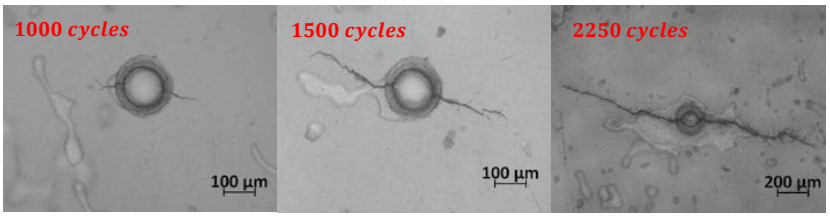

Figure 5 Crack growth measurement near the micro hole

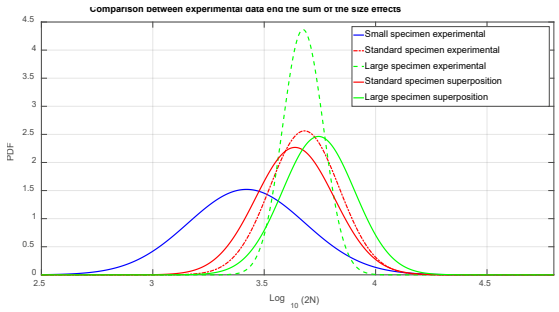

Figure 6. Comparison between extracted distribution and experimental ones

Table 3 Mean and scatter of the life cycles at $\epsilon_a = 0.5\%$ due to the combination of propagation and statistical distribution of defects

		Experimental / $log_{10}(Cycle)$	Extracted / $log_{10}(Cycle)$	μ% error
Standard spec.	Mean	3.6807	3.6382	1.15%
	Std.	0.1557	0.1759	
Large spec.	Mean	3.7021	3.7441	1.13%
	Std.	0.0779	0.1620	

4. Numerical modeling of multiple fracture

As aforementioned, the weakest-link theory assumed that the critical defects do not interact which are sparsely distributed. This assumption only works under limited number of potentially critical defect sites. As noticed from Figure 4, the presence of multiple surface cracks scatted over the gauge section is the main manifestation of damages in 30NiCrMoV12 steel under cyclic loadings. In particular, its fracture was induced by the processes of initiation, growth and coalescence of cracks. Combining with the replica tests as mentioned in Section 2, a numerical Monte Carlo simulation is performed for multiple fracture evaluation and to compare experimental data on crack length distribution evolution, as well as their experimental lives, with the simulated ones.

4.1. Initial prerequisites of the model

The simulation conducted in this analysis includes the process of random crack initiation, propagation and coalescence of surface microcracks occurring simultaneously. According to available experimental data on replica tests under cyclic loadings, the initial prerequisites and assumptions are taken as follows.

(1) Uniform material properties are assumed over the entire damaged surface, namely, the simulation surface area;
(2) Uniaxial stress state is loaded and time-independent during the crack evolution;
(3) All cracks on the surface are oriented normally to the stress action direction, like the *x*-axis in this analysis;
(4) A constant increment of the load cycles is assigned as the count number of iterations;
(5) The positions of all cracks on the surface are randomly distributed according to Poisson's law. Particularly, the probability that n cracks are located on the area A with the crack density λ

$$P(n) = \frac{(-\lambda A)^n}{n!} exp(-\lambda A) \tag{12}$$

(6) The initial length a of the crack is assigned by a two-parameter Weibull distribution;

$$P(a) = 1 - exp\left(-\left(\frac{a-a_0}{\alpha}\right)^{\beta}\right) \tag{13}$$

where β and α are the Weibull shape parameter and scale parameter, which were obtained from measurements on the plastic replicas, and a_0 is the resolution of crack identification.

(7) In crack propagation, the crack length increment for any crack within a given number of iterations is prescribed;
(8) In crack coalescence, quasi-collinear cracks in close proximity interact through the influence zones at both tips, which shows the changes in their propagation paths when their tips approach one another [12]. The influence zone is defined by a circle of diameter r_p according to the size of local plastic deformation zone at the crack tip [13]

$$r_p = \frac{\Delta J_{eff} \cdot E'}{2\pi\sigma_0^2} \tag{14}$$

where ΔJ_{eff} is the effective cyclic J-Integral, σ_0 is the flow stress and E' is the cyclic Young's Modulus under plane strain conditions, $E' = E/(1-v^2)$ and v is the Poisson's ratio.

The criterion of Murakami [14] on judging defects interaction/coalescence is adopted, by the distance between the tips d is less than the minimum of the two crack length

$$d < min(a_{crack1}, a_{crack2}) \tag{15}$$

(9) An unloaded material zone during crack propagation and coalescence is formed around each crack, of which the shape of the zone is defined as a circle of diameter equal to the crack length. In these zones, the crack growth is arrested if its tip comes into the unloading zone from the nearest crack.

Based on abovementioned starting prerequisites, a simulation flow chart is given in Figure 7, the basic inputs obtained from experimental testing for multiple fracture simulation of different geometrical specimens include the following parameters:

(1) Crack density on the surface;
(2) Damage surface size;
(3) Distribution of crack length and crack growth rate (without regard for the crack coalescence) on the surface;
(4) Fracture and failure criterion.

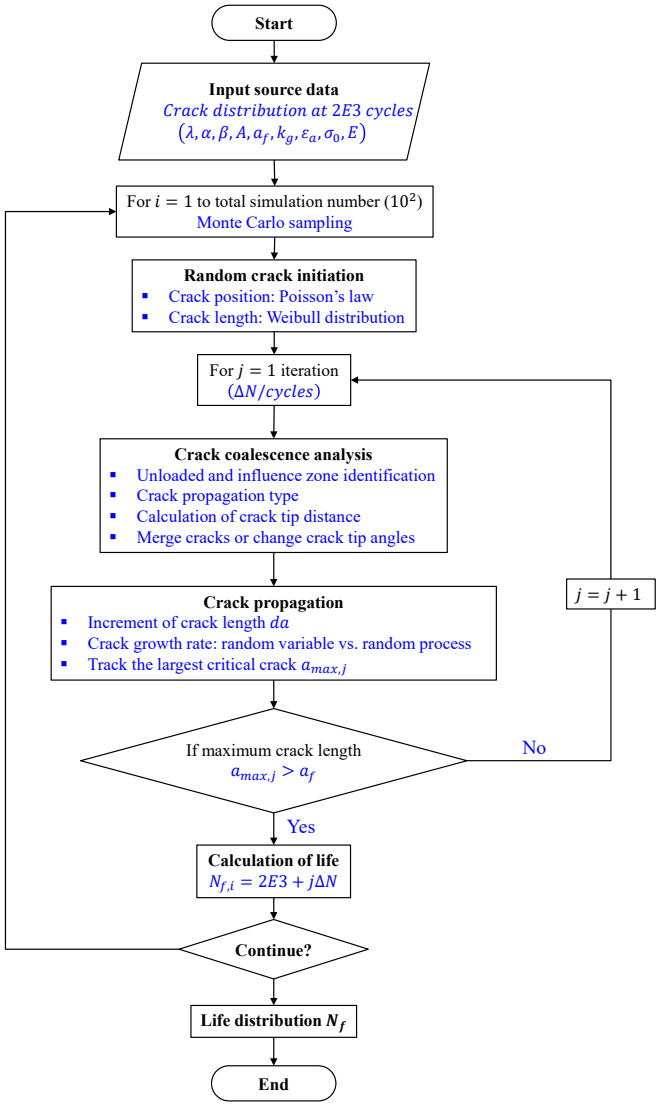

Figure 7. Main flow chart of multiple fracture simulation

4.2. Simulation results and discussions

During simulation, the material damaging under cyclic loading can be characterized by crack initiation, propagation and coalescence, which are dispersed over the surface with different lengths as shown in Figure 8. Two mechanisms of crack propagation, namely, crack length increment due to its own growth for those cracks without coalescence and sudden crack length increment due to the neighbouring cracks coalescence through interacting by their tips, are involved in this simulation. Accordingly, the largest crack exhibits jump-like growth due to merging with other cracks in the plastic radius. Through following the procedure in Section 4.1, an example probability plot of experimental and simulated lives on small specimens is presented in Figure 9. Note that the simulated life distribution covers well with the lives of small specimens except that of G2.13 and G2.14, in which their fracture surfaces in Figure 10 have shown the worst condition on multiple surface crack interaction and propagation.

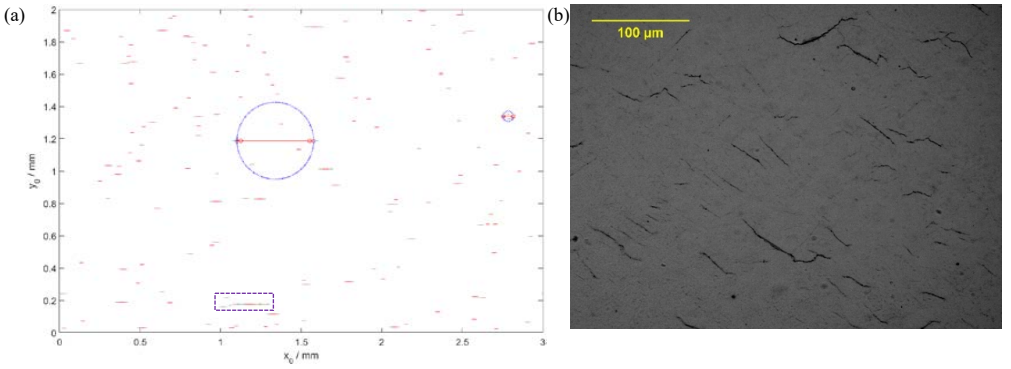

Figure 8. Scheme of crack distribution and unloaded zones (a) Surface crack simulation at $\varepsilon_a = 0.5\%$ (circles mark the unloaded zones, square marks the crack coalescence) and (b) Replica on specimen G 2.12 at 3E3 cycles

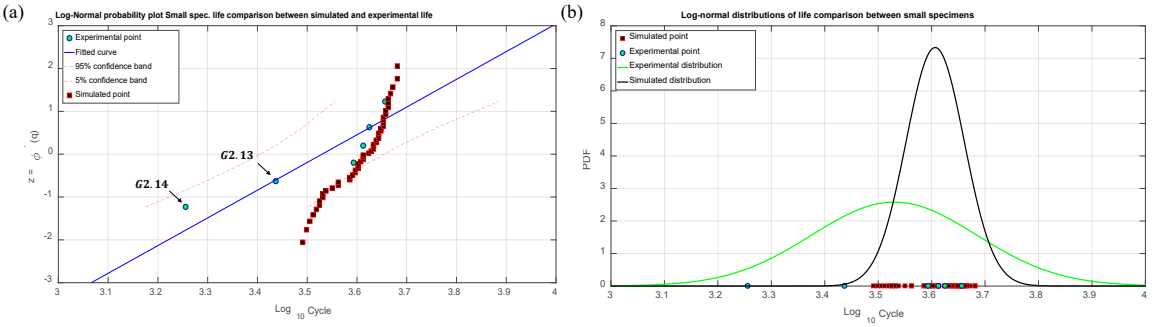

Figure 9. Comparison between experimental and simulated lives of small specimen: (a) probability plot and (b) life distribution

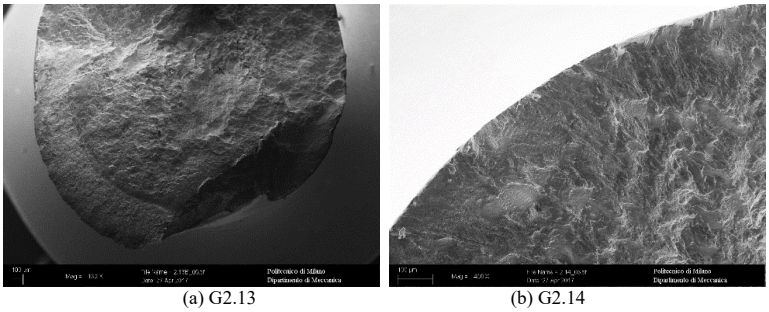

(a) G2.13 (b) G2.14

Figure 10. Fracture surface of small specimens

5. Conclusions

In this study, we proposed a probabilistic modelling and numerical simulation procedure for evaluating the effects of specimen size on fatigue life with three different geometrical specimens. Specifically, the specimen size effect is quantified from two categorizes, namely, size effect due to the effects of statistical defects and crack propagation, which provides a reference for fatigue

life estimation under different specimen sizes. Moreover, a simulation procedure for surface multiple fracture is established by including the random processes of initiation, propagation and coalescence of dispersed surface cracks, which accounts for the observed experimental scatter in fatigue lifetime of small specimen of 30NiCrMoV12 steel. Using this procedure, the life of a component can be predicted from the criterion of critical cracks formation by coalescence of dispersed defects.

Acknowledgments

Dr. S.P. Zhu acknowledges support for his period of study at Politecnico di Milano by the Polimi International Fellowship Grant scheme. The authors acknowledged support by Lucchini RS (Italy) for supplying the heat treated steel.

References

[1] O. Hertel, M. Vormwald, "Statistical and geometrical size effects in notched members based on weakest-link and short-crack modelling," *Eng. Fract. Mech.*, vol. 95, pp. 72–83, 2012.

[2] M. Makkonen, "Statistical size effect in the fatigue limit of steel," *Int. J. Fatigue*, vol. 23, no. 5, pp. 395–402, 2001.

[3] S.P. Zhu, S. Foletti, S. Beretta, "Probabilistic framework for multiaxial LCF assessment under material variability," *Int. J. Fatigue*, in press, https://doi.org/10.1016/j.ijfatigue.2017.06.019, 2017.

[4] T. Tomaszewski, J. Sempruch, T. Piatkowski, "Verification of selected models of the size effect based on high-cycle fatigue testing on mini specimens made of EN AW-6063 Aluminum alloy," *J. Theor. Appl. Mech.*, vol. 52, no. 4, pp. 883–894, 2014.

[5] M. Koyama, H. Li, Y. Hamano, and T. Sawaguchi, "Mechanical-probabilistic evaluation of size effect of fatigue life using data obtained from single smooth specimen : An example using Fe-30Mn-4Si-2Al seismic damper alloy," *Eng. Fail. Anal.*, vol. 72, pp. 34–47, 2017.

[6] Y. Murakami, K. J. Miller, "What is fatigue damage ? A view point from the observation of low cycle fatigue process," *Int. J. Fatigue*, vol. 27, pp. 991–1005, 2005.

[7] "ASTM Standard E606. Standard Practice for Strain-Controlled Fatigue Testing," *Annu. B. ASTM Stand. 3, ASTM Int.*, 2004.

[8] T. S. Hahn, A. R. Marder, "Effect of electropolishing variables on the current density- voltage relationship," *Metallography*, vol. 21, pp. 365–375, 1988.

[9] F. W. Zok, "On weakest link theory and Weibull statistics," *J. Am. Ceram. Soc.*, vol. 100, pp. 1265–1268, 2017.

[10] A. Wormsen, B. Sjödin, G. Härkegård, and A. Fjeldstad, "Non-local stress approach for fatigue assessment based on weakest-link theory and statistics of extremes," *Fatigue Fract. Eng. Mater. Struct.*, vol. 30, no. 12, pp. 1214–1227, 2007.

[11] Tomkins B, "Fatigue crack propagation - an analysis," *Philos. Mag.*, vol. 18, no. 155, pp. 1041–1066, 1968.

[12] H.Y. Yoon, S.C. Lee, "Probabilistic distribution of fatigue crack growth life considering effect of crack coalescence," *JSME Int. J. Ser. A Solid Mech. Mater. Eng.*, vol. 46, no. 4, pp. 607–612, 2003.

[13] S. Rabbolini, S. Beretta, S. Foletti, M. E. Cristea, "Crack closure effects during low cycle fatigue propagation in line pipe steel: An analysis with digital image correlation," *Eng. Fract. Mech.*, vol. 148, pp. 441–456, 2015.

[14] Y. Murakami, *Metal fatigue: effects of small defects and nonmetallic inclusions*. Elsevier, 2002.